A Study on Identification of Ship Type by B-Scope Radar Image using AI

Yasuyuki HIDAKA*, Hideaki NAKAMURA**, Tatsuto YAMADA***,
Naoki MUTA*, Ryotarou OHNO**** and Shinji MIZUI*

* Chuden Engineering Consultants Co.,Ltd, 2-3-30 Deshio,Minami-ku,Hiroshima city, Hiroshima, Japan
** Graduate School of Sciences & Technology for Innovation Yamaguchi University, 2-16-1 Tokiwadai, Ube city, Yamaguchi, Japan
*** Japan Coast Guard Academy, 5-1 Wakaba-cho, Kure city, Hiroshima, Japan
**** Hiroshima National College of Maritime Technology, 4272 Higashino, Oosakikamisima-cho,Hiroshima,,Japan
yhidaka@cecnet.co.jp

Keywords : navigation instruments / measurement, AI technology, radar reflection intensity distribution

ABSTRACT

In a ship traffic survey, it is time taking to identify the type of small ships less than 500 GT those are not required to have AIS on board. Particularly in the nighttime survey when the visibility is limited, time to check the observed record is necessary. Also at night, it is concerned that the observation accuracy might be lower than day time as the identification of ship type tends to depend on the subjective judgement of the observation personnel in nighttime. In this study, aiming at the work and time saving ship traffic survey, we reviewed the possibility of ship type identification by the radar reflection intensity distribution using Artificial Intelligence (AI). At this stage, review on two methods of the ship type identification using AI technology are underway: one by camera images of the ships and the other by the radar reflection intensity distribution. In this paper, we report the result of the review using the radar reflection intensity distribution.

1. Introduction

Before a large-scale construction at sea starts or receiving a large ship at a port as its first call, a traffic survey is performed at the stage to review the safety of the construction or the ship's operation.

In such a survey, traffic volume at the area, operation routes, and the condition of fishing boats in operation at the area are mainly checked. Specifically, in addition to the check of the ship name, type and location using AIS, and the operation routes by installing a shipboard radar at a fixed shore point, a check is also performed by a so called "labor-intensive method" such as visual observation.

This kind of survey is, in many cases, performed by time unit of 24 hours, 48 hours or 72 hours. For the large ships, it is possible to identify the ship structure and type by AIS on board almost around the clock. It is time taking to identify the type and structure of small ships in the nighttime when the visibility is limited, and the time to check the observed record is necessary. Also at night, it is concerned that the observation accuracy might be lower than daytime as the identification of ship type tends to depend on the subjective judgement of the observation personnel.

In this study, aiming at the work and time saving ship traffic survey, we reviewed the possibility of ship type identification by the radar reflection intensity distribution (B scope data) using Artificial Intelligence.

At present, the ship type identification is reviewed by two methods: one by camera image of the ship and the other by the radar reflection intensity distribution using AI.

In this paper, we report the result of the review by the radar reflection intensity distribution.

Table 1 Outline of radar in use

Specification	Antenna part	195cm（24rpm）
	Horizonal beam width	1.2°
	Vertical beam width	22°
	Pulse width	0.3μs (Switch off STC・FTC）
	Transmitting power	12kW
Indicator	Display	15"LCD
	Display cell-size	1024×768 dot
	Distance accuracy	5m
	Range	3NM

2. Observation system

2.1 Observation system of radar reflection intensity

The major specification of the X band radar and the outline of the observation system are shown respectively in Table 1 and Fig.1. This system has a feature of having a mode to output and record the video signals corresponding to the intensity of radar images.

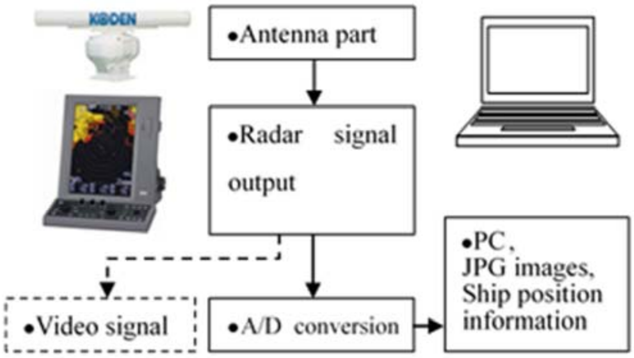

Fig.1 Outline of observation system

As in Fig.1, this system[(1)] has a function to convert the video signals of the shipboard radar by the A/D converter (image converter) and save them in a laptop computer as 12 bits digital data. The image converter incorporates the demodulated signal level converter and the sweep pulse level converting circuit. The output data from the demodulated signal level converter go to the A/D converter, the high-speed buffer memory, the high-speed DIO card and finally to the computer.

2.2 Observed data

The observation of the radar reflection intensity was performed by the afore-mentioned system aboard a small training ship “Hikari” (16 G/T, 17.4m LOA) owned by the National Institute of Technology, Hiroshima College (hereafter called “observation ship”) on September 25, 2021 at the area from Kure Port to Hiroshima Port. The object ships are mainly those under 500 G/T without AIS on board, and the radar reflection intensity was measured 232 times receiving the data from several ships for one observation. During the measurement, the following items were recorded as well: AIS data, photos of the object ships and video footage around those ships, the bearings and distance from the object ships to the observation ship by visual observation and radar, and the type of the ships.

3. Ship type identification system using AI technology

3.1 System outline

The ship type identification is performed using the Convolutional Neural Network (CNN) [(2), (3)] which is one technique of AI. CNN is a kind of the forward propagation neural networks that incorporates a deep layer connecting several convolution layers and pooling layers those consist of a middle layer. The AI determination consists of several programs. For the CNN developed, a model called "VGG-16" which is widely used in the program of the platforms such as the TensorFlow and the Keras that form the base.

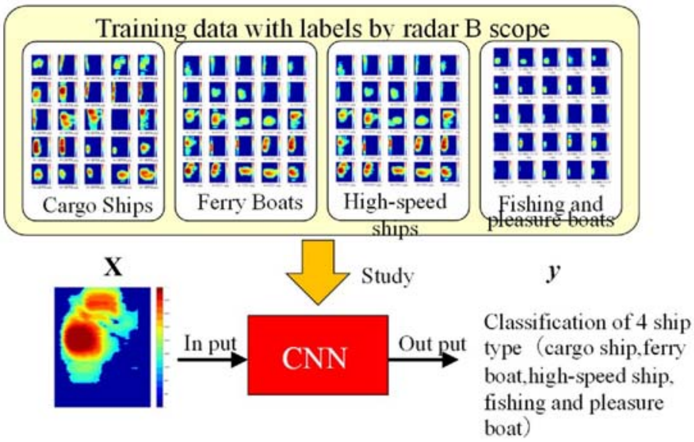

Fig.2 Ship type identification system using CNN

3.2 B scope data

The objects of identification are the following data that include certain amounts of the ship of the same type among the radar reflection intensity distribution data (B scope data) of 232 times as mentioned in Section 2.2.

The number of the object data are 51 from cargo ships including tankers, 51 from ferry boats, 46 from high-speed ships and passenger ships, and 54 from fishing boats both commercial and for pleasure.

The data from other ship types were excluded this time as they did not exceed 20. The data was cross-checked with the record by visual observation and video images to confirm the ship type, and the number of data mentioned above was used for the identification using AI.

The object data are the images of two-dimensional and three-dimensional radar reflection intensity distribution, and the number of object data are 46 to 54 for each of four ship types. Fig.3 shows the case of three-dimensional radar reflection intensity distribution. The horizontal direction of the figure indicates the angle, the longitudinal direction indicates the distance and the height indicates the reflection intensity. The reflection intensity is painted in red for the stronger cases and in blue for the weaker cases. The values of intensity are identical between Fig.3 and Fig.4.The images of three-dimensional radar reflection intensity in Fig.3 are the distribution figures provided that the AD converted values of 900 or under are considered low intensity level and are converted as value zero. The three-dimensional radar reflection distribution in Fig.3 was reviewed, however, it looked differently depending on the observing points. Hence, we used the two-dimensional radar reflection distribution as the object of AI identification in this study and validated the two-dimensional images shown in Fig.4.

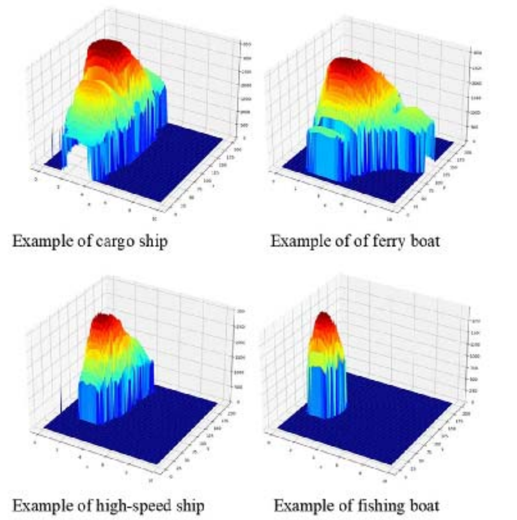

Fig.3 Example of radar reflection intensity data: 3-dimensional distribution

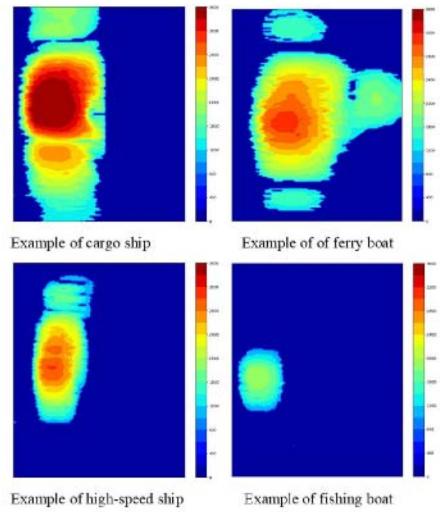

Fig.4 Example of radar reflection intensity data: 2-dimensional distribution

3.3 Measures to improve identification

The number of the observed data are far from enough as 46 to 54. In order to increase the number of learning data, mirror-reversed images were produced for data extension.

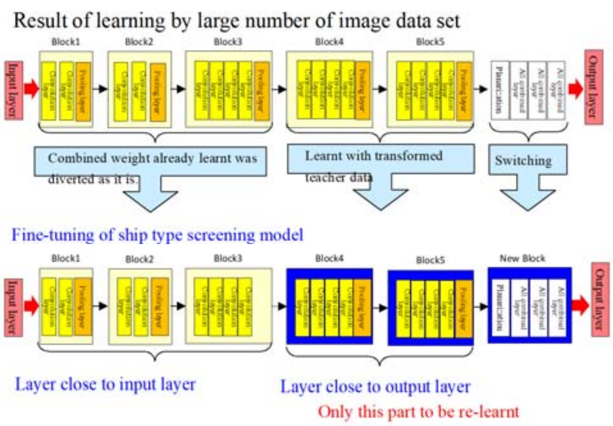

Fig.5 Flow of fine-tuning

As an additional measure to improve the identification with the small number of learning data, the "fine-tuning" was applied to the weight of coefficient which already learnt a large number of image data set called ImageNet. Fine learning is a technology to perform additional learning on a model that has already learnt data of certain field, and customize the model, making the model to accommodate to other field.

The reason why fine-tuning is applied is, in CNN, the low-order and versatile features such as edges are extracted in the layer close to the input layer, meanwhile, the features specialized in the learning data of the task in this study are extracted in the layer close to the output layer. Fig.5 shows the flow of fine-tuning. In this study, as Fig.5 indicates, Block 1 to 3 of "VGG-16" network model are fixed and only Block 4 and 5 are relearnt.

3.4 Correction of reflection intensity by benchmark distance

The radar reflection intensity varies with the factors such as the sea condition, the distance and aspect angle to the object ship. Generally, the most fundamental radar equation is expressed by the formula (1), where p_t is radar transmitting power, G_t is antenna gain, R is distance to the target, σ is radar cross-section (hereafter, RCS) of the target, λ is wavelength, and p_r is radar receiving power. (Interference effect is not considered.)

$$p_r = \frac{p_t \times {G_t}^2 \times \lambda^2 \times \sigma}{(4\pi)^3 \times R^4} \ldots \ (1)$$

The radar receiving power is shown by the following formula since the absolute value of the power setting 1mW as the base is expressed in common logarithm.

$$P_R = 10 \times log_{10}(p_r) = 10 \times log_{10}\{\frac{p_t \times {G_t}^2 \times \lambda^2 \times \sigma}{(4\pi)^3 \times R^4}\} .. \ (2)$$

In order to simplify the process in this study, the formula above is transformed into the following one where only the variation factor by the distance R is focused and the factors except for the distance R including RCS are presumed to be invariant. In this formula, the first term is invariant and the second is variant.

$$P_R = 10 \times log_{10}\left\{\frac{p_t \times {G_t}^2 \times \lambda^2 \times \sigma}{(4\pi)^3}\right\} - 10 \times log_{10}(R^4) \ldots \ (3)$$

The variation volume of the receiving power at the benchmark distance R is shown by the following formula, where the receiving power at a distance r_1 is Pr_1(dBm).

$$P_R - P_{r1} = -10 \times log_{10}(R^4) + 10 \times log_{10}(r1^4) = 10 \times log_{10}(\frac{r1^4}{R^4}) = 40 \times log_{10}\left(\frac{r1}{R}\right) \cdots\cdot \ (4)$$

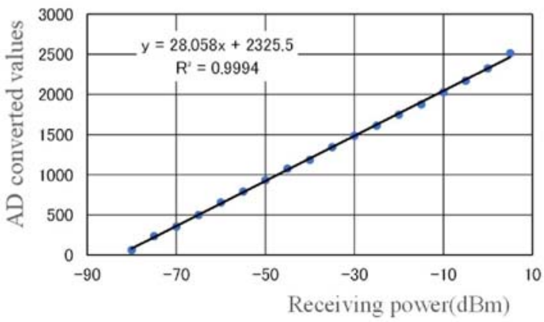

Fig.6 Relation between receiving power and AD converted values

Meanwhile, the calibration test prior to the observation indicates a relation between the receiving power and AD converted values as shown in Fig.6.

This relation makes it possible to calculate the AD converted value at benchmark distance R, if the value gained by multiplying the slope coefficient 28.058 per 1dB of the observed signal intensity with the value obtained by the formula (4) is added or deleted to all the observed AD converted values.

In the observation this time, the average observation distance among 232 times was 1,112m, however, we set R=1,000m as the benchmark distance for easy understanding. The correction of the radar reflection intensity at this distance was performed on all object data.

3.5 Correction of image to angle direction by benchmark distance

The expansion to the angle direction of radar image (reflection intensity distribution) varies as the distance to the observation position varies even for the same ship. Meanwhile, the influence by the distance to the ship is considered small for the enlargement of the images to the distance direction by the pulse width and other factors.

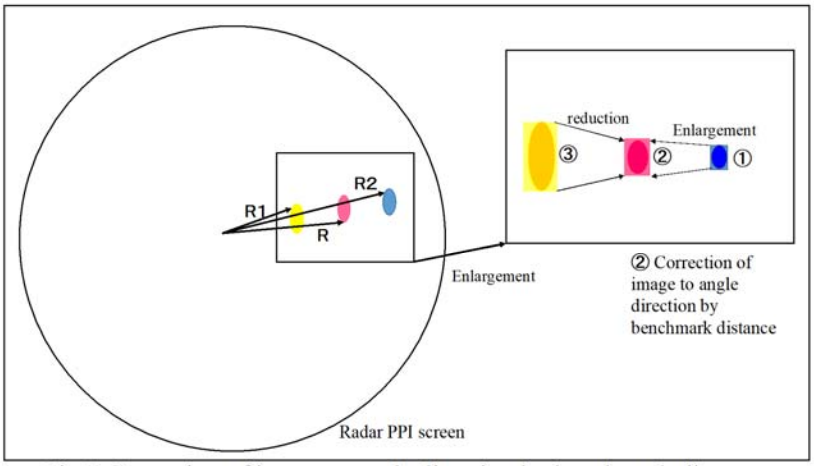

Fig.7 Correction of image to angle direction by benchmark distance

As a result, the shape of the image by angle and distance is to vary with the distance from the observation point and the object ship. This effect is generally called "Echo Paint" on the radar screen.(4) In order to correct the effect by Echo Paint, the expansion of the image to the angle direction was corrected by the ratio between the benchmark distance and the distance to the object ship.

The concept of this correction is explained in Fig.7. The circle on the left in the figure shows the radar PPI screen on which the images of the same ship change from ①(blue simulated image) at a far point, then ②(red simulated image) and to ③(yellow simulated image). This conceptually indicates that there is an enlargement effect on the image of the same ship when it nears. The distance from the ship to R1, R and R2 on the radar screen has a relation that the following formula shows.

$R1 < R < R2 \cdots\cdot$ (5)

According to the relation in the formula (5), scale correction to the angle direction of the images at the benchmark observation distance was performed. That is a reduced scale correction by magnification ratio of R1/R at the observation point ①, and an enlarged scale correction by ratio of R2/R at the point ②.

As stated above, learning and verification data for CNN was prepared by correction to the angle direction of the images, as well as correction of the reflection intensity by the benchmark distance explained in Section 3.4.

4. Result of review and consideration

The ship type identification among four types was performed by the 5-fold cross-validation using the CNN learning indicated in Section 3.1. In the 5-fold cross-validation, all data are divided into 5 groups, and 4 groups out of 5 are used for learning and the remaining 1 is used for validation. This procedure is repeated 5 times using a different group in turn.

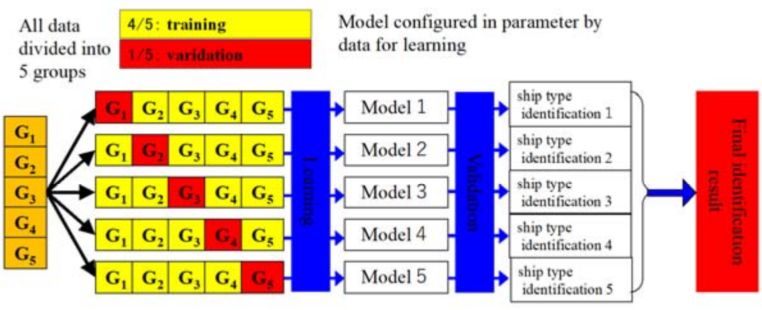

Fig.8 Outline of Final identification result

The identification ratio by ship type among the models from 1 to 5 was validated for each of the 5-fold data in the procedure this time, and the average values of the validation result were summarized in Table 2.

Table 2 summarizes the validation result by ship type in the confusion matrix. The cells in red placed diagonally show the identification ratio. Meanwhile, the remaining 3 cells in white for each type show the misidentification ratio. The identification ratio was 61.4% on average per ship type for 5 validation procedures.

In this review, the identification ratio was not high enough. The following factors are considered to be the reasons and the countermeasures for each factor are required.

Table 2 Result of identification by AI learning

Unit of values in Table: %

	G1 Fishing boat/pleasure boat	G2 Cargo ship	G3 Ferry boat	G4 High-speed ship
G1 Fishing boat/pleasure boat	78.2	10.9	1.8	9.1
G2 Cargo ship	0	58.2	20	21.8
G3 Ferry boat	0	24	56	20
G4 High-speed ship	15.5	4.4	26.6	53.3

(1)The number of observed data is not enough.

(2)The range of data was clipped manually which may cause misidentification errors.

(3)The emission number of sending pulses per rotation of the antenna shows small fluctuations due to the specification of the radar. This causes the errors by fluctuations.

(4) As the data was collected aboard the observation ship underway, the motion of the ship may affect the radar reflection intensity.

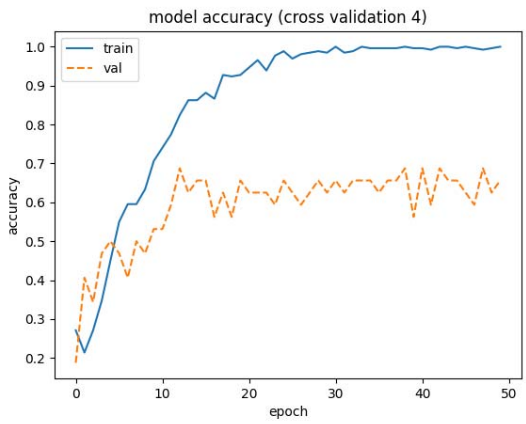

Fig.9 Validation results: Evaluation of accuracy by ship type

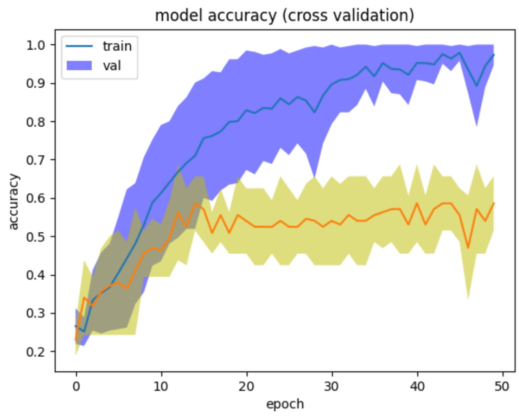

Fig.10 Validation results: Average of accuracy evaluation of 5 times

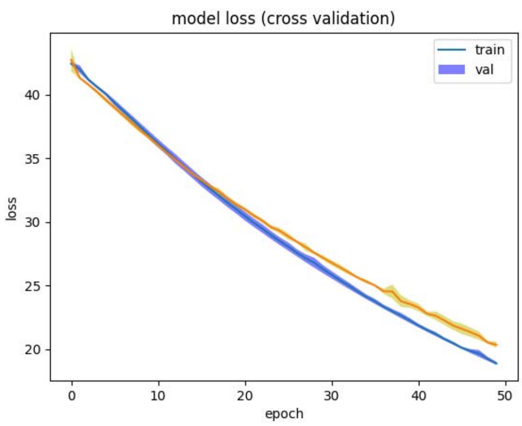

Fig.11 Results of Validation check

The accuracy of AI identification is indicated in Fig.9. Here, the fourth cross-validation result out of 5-fold cross-validation is shown as it marked the best accuracy. The "epoch" on the horizontal axis means the learning times and the "accuracy" on the vertical axis means identification accuracy.

The "train" in blue is the accuracy with the data learnt and the "val" in orange is the accuracy with the data not in use for learning. The accuracy with the data learnt asymptotes 1.0 indicating that the learning is considered successful. On the other hand, the "val", which is the result of validation with the data not in use for learning, asymptotes around 0.6 and the accuracy does not exceed this value. This is considered to be caused by the biased learning and poor generalization performance due to the small number of learning data as previously stated.

Fig.10 indicates all the result of the 5-fold cross-validation showing the range of each validation. The result differs by the combination of the data for learning which is likely to be short in number.

Fig.11 shows the shift of the loss function values (loss errors). As the loss errors gradually decrease, it is considered that the learning proceeds normally.

5. Summary

In this study, a possibility of ship type identification using AI was reviewed. The findings obtained are summarized as follows:

(1) We have established an AI system to identify the ship type with the distribution images of the radar reflection intensity of small ships.

(2) For the determination by the AI system, we have proposed a method to correct the intensity of the radar reflection intensity distribution at the benchmark distance. We also have proposed a method to correct the enlargement of the images.

(3) We have obtained the observation data for one day in September, 2021 at the area from Kure Port to Hiroshima Port. Using these data, we have validated four types of small ships and obtained the identification ratio of 61.4%.

(4) We have sorted the problems to solve for the practical use in the future such as small fluctuations in the number of sending pulse emission per rotation of the antenna. It is necessary to cope with the errors by the fluctuations.

In order to solve the problems summarized as (1) to (4) in Chapter 4, it is needed to increase the number of data by the additional observation at a fixed shore point in the future. We also plan to improve the identification ratio by clipping data range automatically and by measuring the angle interval precisely with accurate counting of the scan pulse signals.

References

(1) Shinji MIZUI,・Tatsuto YAMADA・Akihiro TSUKISAKA and Yoshinori NAKAGAWA (2011) : Analysis of the Two Dimensionally Distributed Radar Echoes of the Small FRP Boat, The Journal of Japan Institute of Navigation, Vol.124, pp.71-77

(2) Alex Krizhevsky・Ilya Sutskever・Geoffrey E,Hinton (2012): ImageNet Classification with Deep Convolutional Neural Networks, Advances in Neural Information Processing Systems (NIPS 2012), pp.1-9,.

(3) K.Simonyan・A.Zisserman (2014): Very deep convolutional networks for large-scale image recognition, arXiv preprint arXiv:1409.1556

(4) Tatsuto YAMADA・Akihiro TSUKISAKA・Shinji MIZUI and Ruri SHOJI (2015): Characteristics of Echo Fluctuation and Echo Paint from the Small FRP Boat on the Marine Radar Screen, International Association of Institutes of Navigation 15th World Congress 2015, IAIN 2015 Congress Proceedings Non-IEEE Full Papers, pp.114-119

Author's Biography

Yasuyuki HIDAKA is currently working as a Manager at Chuden Engineering Consultants Co., Ltd.. His research field is radar signal proceeding and marine traffic engineering, etc.

Hideaki NAKAMURA is a professor of Graduate School of Sciences & Technology for Innovation Yamaguchi University. His research fields are optimization theory, numerical simulation, AI technology and artificial intelligence, etc.

Tatsuto YAMADA is a professor of Japan Coast Guard Academy. His research interests include marine traffic engineering and electronic navigation, etc.

Naoki MUTA is currently working at Chuden Engineering Consultants Co., Ltd.. His research field is radar signal proceeding and marine traffic engineering, etc.

Ryotarou OHNO is a research assistant of National Institute of Technology, Hiroshima College. His research field is ship handling, radar signal proceeding and marine traffic engineering, etc.

Shinji MIZUI is currently working at Chuden Engineering Consultants Co., Ltd.. His research field is maritime transportation, ocean environment, radar signal proceeding and marine traffic engineering, etc.